QUALITATIVE THEORY OF DYNAMICAL SYSTEMS **5**, 75–100 (2004)
ARTICLE NO. 76

Symbolic Dynamics in the Symmetric Collinear Four–Body Problem

Ernesto A. Lacomba and Mario Medina

Mathematics Department,UAM-I. P.O.Box 55-534, México, D.F. 09340
E-mail: lace@xanum.uam.mx, mvmg@xanum.uam.mx

In this article we prove the existence of a countable number of ejection–collision orbits for the symmetric collinear four body problem with negative energy. These orbits come out from total collision, pass through a finite sequence of binary and/or simultaneous binary collisions and finally end in total collision. The existence of this family of orbits relies on the existence of the homothetic orbit joining the pair of hyperbolic equilibrium points lying on the total collision manifold and on the knowledge of the flow on the total collision manifold.

Key Words: Celestial mechanics, symbolic dynamics, total collision manifold, collisions.

1. INTRODUCTION

We study a two degrees of freedom problem in celestial mechanics, the collinear symmetric four body problem, which depends on one positive parameter given in terms of the masses of the particles. In [5], Lacomba and Simó introduced this problem and obtained valuable information about the nature of the flow on the total collision manifold M, the flow varies according the value of the parameter and for values of the parameter in some open intervals the obtained flow on the total collision manifold turned out to be very symmetric as we can see in Figure 2. The branches of the unstable manifold associated to the equilibrium point c restricted to M act as separatrices and escape through different upper arms of M after giving the same number of turns around it. This feature and the existence of the homothetic orbit are fundamental for proving the existence of the desired family of orbits. For values of the parameter outside the considered intervals the flow may not be symmetric and we can not use the developed methods to assure the existence of the family of orbits.

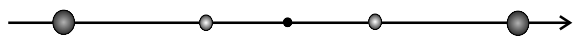

FIG. 1. Symmetric Collinear Four–Body Configuration.

2. STATEMENT OF THE PROBLEM

Consider four particles forming a collinear configuration, placed symmetrically by pairs, respect to the center of mass, which is the origin, see Figure 1. Assume that each one of the particles of the inner pair have mass 1 and each particle of the exterior pair have mass α. Initial conditions for the set of masses are such that the symmetric configuration is preserved as the full system evolves under newtonian attraction.

Let $m_1 = m_2 = 1$, $m_3 = m_4 = \alpha$ be the masses of the particles and $x, -x, y/\sqrt{\alpha}, -y/\sqrt{\alpha}$ be their coordinates.

The configuration space is given by the subset of the first quadrant defined by

$$\mathbf{Q} = \{(x, y) \in \mathbf{R}^2 \ \mid \ x, y > 0 \ \text{ and } \ \sqrt{\alpha}x < y\}.$$

Observe that the set of points $\mathbf{q} = (0, y)$ with $y \neq 0$ correspond to binary collisions of the inner pair of particles; while the set of points $\mathbf{q} = (x, y)$ with $y = \sqrt{\alpha}x \neq 0$ correspond to symmetric binary collisions and the point $\mathbf{q} = (x, y) = (0, 0)$ corresponds to total collision of the four particles.

We write down the Lagrangian of the system

$$L = T + U,$$

where $T(x, y) = \dot{x}^2 + \frac{\dot{y}^2}{\alpha}$ is the kinetic energy and $U(x, y) = \frac{1}{2x} + \frac{\alpha^{5/2}}{2y} + \frac{2\alpha^{3/2}}{y-\sqrt{\alpha}x} + \frac{2\alpha^{3/2}}{y+\sqrt{\alpha}x} = \frac{1}{2x} + \frac{\alpha^{5/2}}{2y} + \frac{4\alpha^{3/2}y}{y^2-\alpha x^2}$ is the potential energy .

The generalized momenta are given by

$$p_x = \frac{\partial L}{\partial \dot{x}} = 2\dot{x}, \quad p_y = \frac{\partial L}{\partial \dot{y}} = \frac{2\dot{y}}{\alpha}, \tag{1}$$

where $\dot{} = \frac{d}{dt}$.

By denoting $\mathbf{p} = (p_x \ p_y)^t$, $\quad \mathbf{q} = (x \ y)^t \quad$ y $\quad \dot{\mathbf{q}} = (\dot{x} \ \dot{y})^t$, the Hamiltonian is

$$\begin{aligned} H &= \mathbf{p}^t\dot{\mathbf{q}} - L(\mathbf{q}, \dot{\mathbf{q}}) \\ &= \frac{1}{4}({p^2}_x + \alpha {p^2}_y) - \frac{1}{2x} - \frac{\alpha^{5/2}}{2y} - \frac{2\alpha^{3/2}}{y - \sqrt{\alpha}x} - \frac{2\alpha^{3/2}}{y + \sqrt{\alpha}x} \end{aligned}$$

$$= \frac{1}{4}({p^2}_x + \alpha {p^2}_y) - U(x,y),$$

and the equations of motion are

$$\dot{\mathbf{q}} = \frac{\partial H}{\partial \mathbf{p}}, \quad \dot{\mathbf{p}} = -\frac{\partial H}{\partial \mathbf{q}}, \tag{2}$$

which are written as

$$\begin{aligned} \dot{x} &= \tfrac{p_x}{2}, \quad \dot{p}_x = -\tfrac{1}{2x^2} + \tfrac{8\alpha^{5/2}xy}{(y^2-\alpha x^2)^2}, \\ \dot{y} &= \alpha\tfrac{p_y}{2}, \ \dot{p}_y = -\tfrac{\alpha^{5/2}}{2y^2} - 4\alpha^{3/2}\tfrac{y^2+\alpha x^2}{(y^2-\alpha x^2)^2}. \end{aligned} \tag{3}$$

Next, by using the blow-up technique introduced by McGehee [4], we can describe the total collision manifold and the flow on this invariant manifold. Using this information of the flow on the total collision manifold it is possible to give a description of the flow near the total collision manifold.

Let $\mathbf{I} = \mathbf{q}^t\mathbf{q}$ be the moment of inertia. We define the blow-up of the origin by the following change of coordinates,

$$r = \mathbf{I}^{\frac{1}{2}}, \ \mathbf{s} = r^{-1}\mathbf{q}$$

where r measures the size of the system and $\mathbf{s}$ is the configuration or shape of the system. $S = \{\mathbf{q} \in \mathbf{Q} \mid r = 1\}$ is a unit sphere in $\mathbf{Q}$. Coordinates $(r, \mathbf{q})$ represent a polar-like system of coordinates for the configuration space. It is clear that $\mathbf{s}^t\mathbf{s} = 1$.

If $\mathbf{u}$ and v are the (rescaled) tangential and radial components of the momentum given by

$$\mathbf{u} = \sqrt{r}\mathbf{p} - (\mathbf{p}^t\mathbf{s})\mathbf{s}, \quad v = \sqrt{r}\mathbf{p}^t\mathbf{s}$$

with the time reparametrization

$$\frac{dt}{d\tau} = r^{\frac{3}{2}},$$

the equations of motion become

$$\begin{aligned} \dot{r} &= rv, \\ \dot{v} &= \mathbf{u}^t\mathbf{u} + \frac{v^2}{2} + U(\mathbf{s}), \\ \dot{\mathbf{s}} &= \mathbf{u}, \\ \dot{\mathbf{u}} &= -\frac{1}{2}v\mathbf{u} - (\mathbf{u}^t\mathbf{u})\mathbf{s} + Grad\ U(\mathbf{s}), \end{aligned}$$

and the energy relation $H = h$ is rewritten as

$$\frac{1}{2}(\mathbf{u}^t\mathbf{u} + v^2) = U(\mathbf{s}) + rh.$$

As we have a two degree of freedom problem, we use canonical polar coordinates to work with: θ is the usual angular coordinate and the component of the rescaled velocity in the angular direction, which we shall denote by u, through the change

$$\mathbf{s} = (\cos\theta \quad \sin\theta)^t, \quad \mathbf{u} = u(\cos\theta \quad \sin\theta)^t.$$

In coordinates (r, v, θ, u, τ), the equations of motion are expressed by

$$\begin{aligned} r' &= rv, \\ v' &= u^2 + \frac{v^2}{2} - U(\theta), \\ \theta' &= u, \\ u' &= -\frac{1}{2}vu + \frac{dU(\theta)}{d\theta}, \end{aligned} \tag{4}$$

where $' = \frac{d}{d\tau}$. In the same way, the energy relation is transformed into

$$\frac{1}{2}(u^2 + v^2) = U(\theta) + rh,$$

where $U(\theta) = \frac{1}{2\cos\theta} + \frac{\alpha^{5/2}}{2\sin\theta} + \frac{4\alpha^{3/2}\sin\theta}{\sin^2\theta - \alpha\cos^2\theta}$, $\theta \in (\theta_\alpha, \pi/2)$.

Our equations still have singularities when the particles of the inner pair collide or when we have symmetric simultaneous binary collisions, that is, when $\theta = \pi/2$ or $\theta = \theta_\alpha$, where $\tan\theta_\alpha = \sqrt{\alpha}$.

In order to simultaneously regularize these singularities, consider the function $W(\theta) = U(\theta)\cos\theta(\sin\theta - \sqrt{\alpha}\cos\theta)$, a new variable

$$w = \frac{\cos\theta(\sin\theta - \sqrt{\alpha}\cos\theta)}{2\sqrt{W(\theta)}}u,$$

with the time rescaling

$$\frac{d\tau}{ds} = \frac{\cos\theta(\sin\theta - \sqrt{\alpha}\cos\theta)}{2\sqrt{W(\theta)}}.$$

The equations of motion and the energy relation become

$$
\begin{aligned}
\frac{dr}{ds} &= rv\frac{\cos\theta(\sin\theta-\sqrt{\alpha}\cos\theta)}{2\sqrt{W(\theta)}},\\
\frac{dv}{ds} &= \frac{\sqrt{W(\theta)}}{2}\{(2rh-\frac{1}{2}v^2)\frac{\cos\theta(\sin\theta-\sqrt{\alpha}\cos\theta)}{\sqrt{W(\theta)}}+1\},\\
\frac{d\theta}{ds} &= w,\\
\frac{dw}{ds} &= (\cos\theta(\sin\theta-\sqrt{\alpha}\cos\theta)-w^2)\frac{\frac{dW}{d\theta}}{2W(\theta)}-\frac{vw\cos\theta(\sin\theta-\sqrt{\alpha}\cos\theta)}{2\sqrt{2W(\theta)}}\\
&\quad+\frac{(\cos(2\theta)+\sqrt{\alpha}\sin(2\theta))}{2}\{3+\frac{2rh-v^2}{W(\theta)}\cos\theta(\sin\theta-\sqrt{\alpha}\cos\theta)\}
\end{aligned}
$$

and

$$w^2=\frac{\cos^2\theta(\sin\theta-\sqrt{\alpha}\cos\theta)^2}{4W(\theta)}(2rh-v^2)+\frac{\cos\theta(\sin\theta-\sqrt{\alpha}\cos\theta)}{2},$$

respectively. Taking $r=0$ in last equation, this can be rewritten as

$$w^2=\frac{\cos\theta(\sin\theta-\sqrt{\alpha}\cos\theta)}{2}-\frac{v^2\cos^2\theta(\sin\theta-\sqrt{\alpha}\cos\theta)^2}{4W(\theta)}. \tag{5}$$

In this way we have extended the vector field to the components determined by binary and simultaneous binary collisions. We define the total collision manifold as the set

$$M=\{(r,v,\theta,w)\ \mid\ r=0,\ \text{equation (5) holds, and } \theta_\alpha\le\theta\le\pi/2\}.$$

3. DESCRIPTION OF THE FLOW ON THE TOTAL COLLISION MANIFOLD

Next we give some features of the flow on the total collision manifold obtained by using the blow up technique.

For a value of the parameter α, the equilibrium points are $(r=0, v=\pm\sqrt{U(\tilde{\theta}_\alpha)}, \theta=\tilde{\theta}_\alpha, w=0)$, which lie on the total collision manifold M. All equilibrium points are hyperbolic. Also, the flow on the total collision manifold is almost gradient with respect to v. In Figure 2 we show the flow on the total collision manifold for different values of α as obtained in [5].

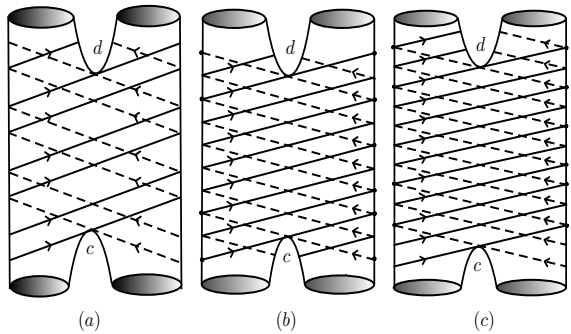

FIG. 2. Flow on the total collision manifold, (a) $0 < \alpha < \alpha_1$, (b) $\alpha_2 < \alpha < \alpha_3$ and (c) $\alpha_3 < \alpha < \alpha_4$.

TABLE 1.
Dimensions of invariant manifolds for the equilibrium points in $\boldsymbol{M}$

	Invariant		Manifolds	
	$\overline{W}^u(d)$	$\overline{W}^s(d)$	$\overline{W}^u(c)$	$\overline{W}^s(c)$
Dimension	2	1	1	2
	$W^u(d)$	$W^s(d)$	$W^u(c)$	$W^s(c)$
Dimension	1	1	1	1

For each value of α there are two hyperbolic equilibrium points, one of them corresponds to a positive value of v, while the other corresponds to a negative value of v.

We denote by $\overline{W}^{s,u}$ the stable and unstable manifolds associated to an equilibrium point, for a negative value of energy h. $W^{s,u} = \overline{W}^{s,u} \cap M$ will denote the intersection of the stable and unstable manifolds of equilibrium points with the total collision manifold.

Dimensions of the invariant manifolds associated to each hyperbolic point c and d on M are given in Table 1. Notice that all the $W^{u,s}$ are one dimensional, so they act as separatrices of the flow on M.

We are interested in values of the parameter contained in some open intervals for which the flow on the total collision manifold is symmetric as in Figure 2. We exclude other values of the parameter as those given for bifurcation values and some open intervals, since in these cases there are two situations where we can not apply the ideas we develop in the symmetric cases: (i) one or both of the separatrices $W^u(c)$ coincide with one or both separatrices $W^s(d)$ or (ii) both separatrices $W^u(c)$ escape through

the same upper arm of M. In [5] page 61, the authors obtained several bifurcation values for α, (α_k, $\alpha_i < \alpha_{i+1}$), and in consequence, intervals defined by these parameter values. The intervals we are interested in are intervals like $(0, \alpha_1), (\alpha_2, \alpha_3)$ and (α_3, α_4). For values in these intervals the corresponding flow is as given in Figure 2, rather symmetric.

4. EXISTENCE OF THE HOMOTHETIC ORBIT

For negative values of the energy h we shall prove the existence of a homothetic orbit contained in $\overline{W}^s(c) \cap \overline{W}^u(d)$, located outside the total collision manifold and joining the equilibrium points c and d. This homothetic orbit will be of great importance in order to give the desired description of the family of orbits which come out from total collision, pass through a sequence of binary collisions of the particles of the inner pair and/or simultaneous binary collisions, and finally end in total collision.

Recall that homothetic solutions are characterized by the fact that $\theta \equiv \tilde{\theta}_\alpha$, where $U'(\tilde{\theta}_\alpha) = 0$. By using system (4) of equations, we can obtain a parametric representation of the homothetic orbit. When $\theta \equiv \tilde{\theta}_\alpha$, then $u = 0$ and, in consequence we have equations

$$\frac{dr}{d\tau} = rv, \quad \frac{dv}{d\tau} = \frac{v^2}{2} - U(\tilde{\theta}_\alpha),$$

so,

$$\frac{dv}{2U(\tilde{\theta}_\alpha) - v^2} = \frac{d\tau}{-2},$$

taking $v_\alpha = \sqrt{2U(\tilde{\theta}_\alpha)}$, we get

$$\tanh^{-1}(\frac{v}{v_\alpha}) = -\frac{\tau v_\alpha}{2},$$

that is

$$v(\tau) = -v_\alpha \tanh(\tau v_\alpha/2).$$

Using the expression for $v(\tau)$, we obtain

$$r(\tau) = -\frac{U(\tilde{\theta}_\alpha)}{h \cosh^2(\tau v_\alpha/2)}.$$

Also, we can give a geometrical description of the homothetic orbits. In system (4), by using the energy relation $\frac{1}{2}(u^2+v^2) = U(\theta)+rh$, with $u = 0$, we obtain

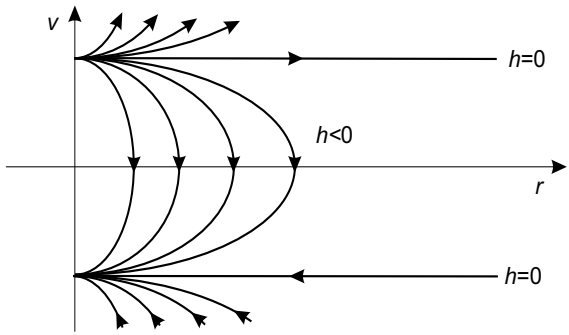

FIG. 3. Homothetic orbits in the plane $u = 0, \theta = \tilde{\theta}_\alpha$.

$$\frac{dr}{d\tau} = rv, \frac{dv}{d\tau} = rh.$$

By solving this system of differential equations, we get

$$v^2 = 2rh + m.$$

These solutions can be seen as restrictions of the energy relation to the plane $u = 0, \theta = \tilde{\theta}_\alpha$; that is $\frac{v^2}{2} = rh + U(\tilde{\theta}_\alpha)$, so we have $m = 2U(\tilde{\theta}_\alpha)$. For each negative value of h, we have an orbit coming out from one of the equilibrium points and ending at the other equilibrium point, as seen in Figure 3.

Definition 1. We say that an orbit having c as ω-limit is an orbit which *ends in total collision* or a *total collision orbit* and an orbit having d as α-limit is an *ejection orbit* or an orbit *coming out from total collision.*

In this way, all orbits contained in $\overline{W}^u(d)$ are ejection orbits and those contained in $\overline{W}^s(c)$ are total collision orbits. Orbits contained in $\overline{W}^s(c) \cap \overline{W}^u(d)$ will be called *ejection-collision orbits.*

5. POINCARÉ-SECTION AND BASIC RESULTS

We proceed to construct a Poincaré-section for the flow in order to analyze how an orbit can pass through binary collision of the inner pair or through a simultaneous binary collision. It is important to have in mind that coordinate w must be equal to zero.

We define the set

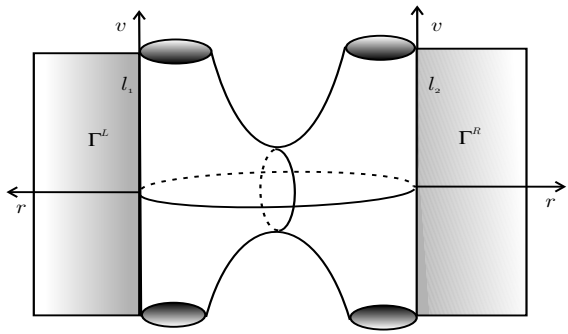

FIG. 4. Section of binary and simultaneous binary collisions

$$\Gamma = \{(r, v, \theta, w) \mid \ r \geq 0, \theta = \theta_\alpha, \pi/2, w = 0\},$$

which is the union of two half-planes,

$$\Gamma^L = \{(r, v, \theta, w) \mid \ r \geq 0, \theta = \theta_\alpha, w = 0\},$$

and

$$\Gamma^R = \{(r, v, \theta, w) \mid \ r \geq 0, \theta = \pi/2, w = 0\},$$

that are parametrized by coordinates $(r, v) \in [0, \infty) \times \mathbf{R}$. See Figure 4.

Observe that lines l_1 and l_2 in Figure 4 correspond to lines $r = 0$ contained in the half-planes Γ^L and Γ^R, respectively.

Now, we obtain the first intersection in positive time of $\overline{W}^u(d)$ with Γ following ideas contained in [2] and [3].

PROPOSITION 2. *The first intersection in positive time of $\overline{W}^u(d)$ and Γ contains two arcs $\sigma^{R,L}$, contained in $\Gamma^{R,L}$ and with extremes on the boundaries of $\Gamma^{R,L}$ (lines l_1 and l_2 respectively).*

Proof. Let dR_* be the first point in positive time in one of the branches of the one-dimensional invariant manifold $W^u(d)$ which is contained in Γ^R. In the same way, define $dL_* \in \Gamma^L$ as the corresponding point contained in the other branch of $W^u(d)$. On the other hand, let cR_* and cL_* be the first points of the unstable branches of $W^u(c)$ contained in Γ^R and Γ^L after ejection of the four particles.

Consider an arc σ of initial conditions near d, contained in $\overline{W}^u(d)$, homeomorphic to a semicircle parametrized by angle $\phi \in [0, \pi]$, in such a way that $\phi = 0$ corresponds to a point $\mathbf{p}$ of the unstable branch of $W^u(d)$ which contains point dR_*; $\phi = \frac{\pi}{2}$ corresponds to a point $\mathbf{q}$ in the homothetic orbit,

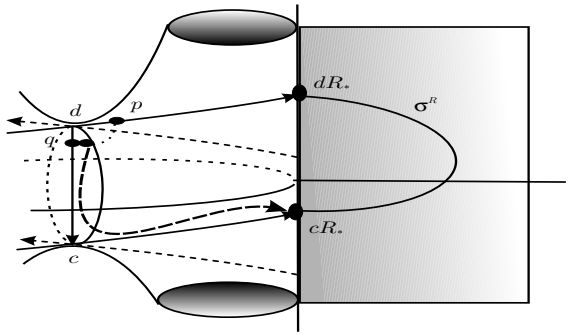

FIG. 5. First intersection in positive time of $\overline{W}^u(d)$ with Γ^R.

and $\phi = \pi$ corresponds to a point $\mathbf{t}$ in the branch of the unstable branch of $W^u(d)$ containing dL_*.

In order to find the first intersection point of $\overline{W}^u(d)$, in positive time, with Γ, we follow the semicircle σ of initial conditions under the flow. First, we consider the segment of the semicircle parametrized by $\phi \in [0, \pi/2]$, so, point $\mathbf{p}$ goes, under the flow, to point $dR_* \in \Gamma^R$ and points in this subarc, near $\mathbf{p}$ go to points in Γ^R, near dR_*; on the other hand, points near $\mathbf{q}$ go near c and, then, continuing near the unstable branch of c, pass close to cR_*. The subarc of σ, parametrized by $[0, \pi/2]$, being a continuous arc, its image under the flow must be a continuous arc which we denote by σ^R, and is contained in Γ^R. Its extremes are denoted by dR_* and cR_*, as shown in Figure 5. In an analogous way, the image of the subarc parametrized by $[\pi/2, \pi]$ is also a continuous arc σ^L, contained in Γ^L, with extremes dL_* and cL_* in line $\{r = 0\} \cap \Gamma^L$. ▌

Let R_*d and L_*d be those points on the stable branches of $W^s(d)$, contained in Γ^R and Γ^L that go to d, but such that no other point in their positive time orbits are contained in Γ^R or Γ^L. In the same way we define points $R_*c \in \Gamma^R$ and $L_*c \in \Gamma^L$ as those points in $W^s(c)$, so that their positive time orbits do not intersect Γ^R nor Γ^L.

PROPOSITION 3. *The last intersection, in positive time of $\overline{W}^s(c)$ with Γ is given by two arcs $\gamma^{R,L}$, contained in $\Gamma^{R,L}$, whose extremes (of the arcs) given by R_*d, R_*c and L_*d, L_*c are contained on the boundary of $\Gamma^{R,L}$ (lines l_1 and l_2, respectively).*

Proof. Using the symmetry given by the reversibility of the original Hamiltonian system for the symmetric collinear four body problem and

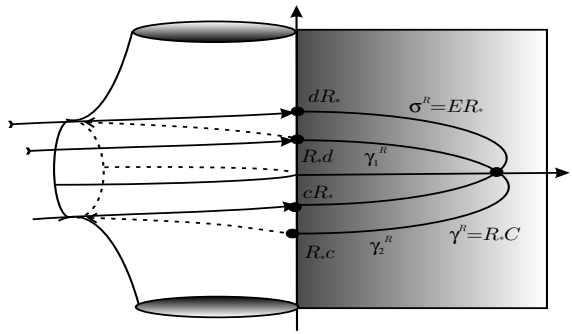

FIG. 6. Point of intersection corresponding to an ejection-collision orbit.

which, when restricted to Γ, is represented by

$$(r, v, t) \longrightarrow (r, -v, -t),$$

we obtain that, the set of initial conditions in $\overline{W}^s(c)$, whose positive orbits do not intersect Γ is given by the reflection of $\sigma^{R,L}$ in Γ, with respect to the half lines $v = 0$, obtaining arcs $\gamma^{R,L} \subset \Gamma^{R,L}$, which have extremes given by points R_*d, R_*c and L_*d, L_*c, respectively, as shown in Figure 6. ▌

Denote arc σ^R by ER_*, this notation means that all points on this arc come out from total collision and then intersect Γ^R. Their trajectories eject away from total collapse and then reach a *right* binary collision, i.e. of the inner pair. In a similar way, we shall denote arc σ^L by EL_*, obtaining trajectories that eject from total collision and then they pass through a *left* or simultaneous binary collision. Also, arc γ^R, obtained in last proposition, will be denoted by R_*C, since orbits through these points intersect Γ^R transversally, passing through a *right* binary collision and finally reaching total collision, without having another binary or simultaneous binary collision. Analogously, arc γ^L shall be denoted by L_*C. In general, if an orbit intersects Γ^R or Γ^L, we will say that at the time the orbit intersects these sets the orbit passes through a *right*–binary collision (*right*–BC) or a *left*–simultaneous binary collision (*left*–SBC).

In this way, it can be shown that the pair $\sigma^R, \gamma^R \subset \Gamma^R$ intersect, at least in one point, as we see in Figure 6, contained in $\overline{W}^u(d) \cap \overline{W}^s(c)$. To these points correspond ejection-collision orbits having a *right* binary collision (*right*–BC). A similar argument shows that to points contained in the intersection $\sigma^L \cap \gamma^L$ correspond trajectories having a *left* simultaneous binary collision (*left*–SBC).

To each one of these ejection-collision orbits having a *right*–BC (*left*–SBC) we associate a sequence of symbols of the form ERC (ELC), which means that these orbits eject from total collision, pass through a *right*–BC (*left*–SBC) and then go directly to total collision without having another binary or simultaneous binary collision.

Next, we characterize the pullbacks of $\overline{W}^s(c) \cap \Gamma$ under the Poincaré map

$$P : \Gamma \longrightarrow \Gamma$$

also known as the first return map which is defined as follows. Let p a point in Γ so that its positive orbit $\phi(t, p)$ intersects Γ transversally at time T and $\phi(t, p)$, for $t \in (0, T)$, does not intersect Γ; for points in Γ near p their trajectories return to Γ in time close to T. The map associates to points x in Γ near p their points of first return to Γ. To be more precise, for x in Γ close to p

$$P(x) = \phi(\tau(x), x)$$

where $\tau(x)$ is the time of first return of the orbit through point x to Γ.

The following results will be of fundamental importance for characterizing all orbits passing through binary or simultaneous binary collisions.

Proposition 4.

1.If σ is a subsegment in $\overline{W}^s(c) \cap \Gamma$, having points A and B on $\{r = 0\}$ as extremes, in such a way that it does not intersect $\overline{W}^u(d)$, then $P^{-1}(\sigma)$ is an arc contained in Γ with extreme points $P^{-1}(A)$ and $P^{-1}(B)$ on M.

2.If σ is a subsegment in $\overline{W}^s(c) \cap \Gamma$, with ends A and B on $\{r = 0\}$ such that it intersects $\overline{W}^u(d)$, then the pullback of subsegment $\widetilde{\sigma}$ on σ that lies between point A and the first intersection point of σ with $\overline{W}^u(d)$ is a segment contained in Γ, that has as extreme points $P^{-1}(A)$ and R_*d or L_*d depending on which half-plane of Γ lies point $P^{-1}(A)$.

3.If γ is an arc in $\overline{W}^s(c) \cap \Gamma$ that contains a subarc $\widetilde{\gamma}$, with ends on $\overline{W}^u(d)$ and such that no other point on this subarc lies on $\overline{W}^u(d)$, then the pullback of $\widetilde{\gamma}$ is a loop on Γ with extremes on (i) L_*d if segment $\widetilde{\gamma}$ pulls back to Γ^R, or (ii) R_*d if segment $\widetilde{\gamma}$ pulls back to Γ^L.

Proof.

1. Consider arc σ with points A and B on $\{r = 0\}$ as extremes, and denote the pullbacks of these extremes by $P^{-1}(A)$ and $P^{-1}(B)$. By continuity, points contained in σ near A, under the flow, go to points near $P^{-1}(A)$. There is a problem if there exists a point on $\sigma \cap \overline{W}^u(d)$, because in this case, this point would correspond to a ejection point, but this is not the case by hypothesis. So, $P^{-1}(\sigma)$ is a subarc contained in Γ with extreme points given by $P^{-1}(A)$ y $P^{-1}(B)$. See Figure 7.

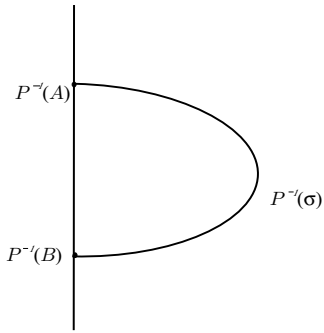

FIG. 7. Pullback of an arc segment in Proposition 4, case 1.

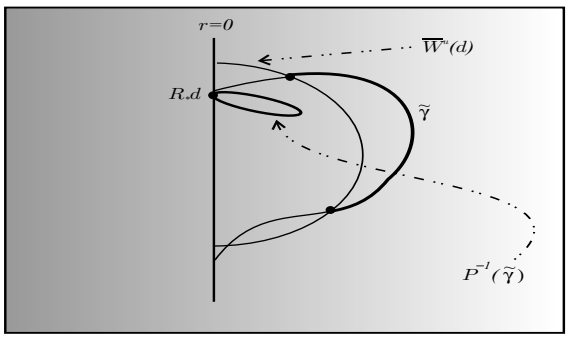

FIG. 8. Pullback of an arc segment in Proposition 4, case 3.

2. Let σ be a segment in $\overline{W}^s(c) \cap \Gamma$ with extreme points A and B on $\{r = 0\}$, such that it intersects $\overline{W}^u(d)$ and let $\widetilde{\sigma} \subset \sigma$ be an arc with A as one extreme and the other extreme given by the first intersection of σ with $\overline{W}^u(d)$. Point A pulls back to $P^{-1}(A)$ and points on $\widetilde{\sigma}$ near A, pull back to points near $P^{-1}(A)$; we continue pulling back points in $\widetilde{\sigma}$ until we are near the intersection of $\widetilde{\sigma}$ with $W^u(d)$; under the flow in negative time, they must be close enough to the equilibrium point d, so they must pass through Γ near L_*d or R_*d. Therefore, $P^{-1}(\widetilde{\sigma})$ in an arc contained in Γ joining points $P^{-1}(A)$ and R_*d or L_*d, depending on which half plane of Γ the point $P^{-1}(A)$ lies.

3. By continuity, the pullback of the whole arc $\widetilde{\gamma}$, must be completely contained in one of the half planes Γ^R or Γ^L. By a similar argument to the one given in last paragraph, following under the flow in negative time points on $\widetilde{\gamma}$ near $\overline{W}^u(d)$, we get close to d, so their orbits intersect Γ in

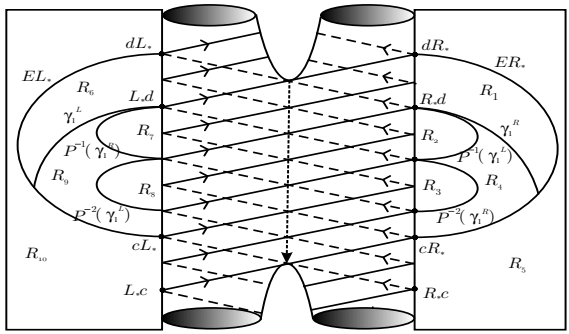

FIG. 9. Pullback of an arc segment in Corollary 5, case (2).

points near the stable branches of d contained in M; that is, must pass close to R_*d or L_*d. But the pullback of $\widetilde{\gamma}$ is entirely contained in the same half plane, so the pullback is a loop with extremes in R_*d or L_*d as we can see in Figure 8.

∎

COROLLARY 5. *Let ζ be an arc contained in $\overline{W}^s(c) \cap \Gamma^R$ with point R_*d and arc ER_* as extremes, so that no other point in the arc is contained in ER_*. Then,*

1.For $0 < \alpha < \alpha_1$, $P^{-2}(\zeta)$ is an arc in Γ^R with extremes $P^{-1}(L_*d)$ and $P^{-2}(R_*d)$ which intersects ER_*, but $P^{-1}(\zeta)$ does not intersect EL_*.

2.For $\alpha_2 < \alpha < \alpha_3$, $P^{-3}(\zeta)$ is an arc in Γ^L with extremes $P^{-2}(L_*d)$ and $P^{-3}(R_*d)$ which intersects EL_*, but $P^{-1}(\zeta)$ and $P^{-2}(\zeta)$ do not intersect EL_* or ER_*, respectively.

3.For $\alpha_3 < \alpha$, $P^{-4}(\zeta)$ is an arc in Γ^R with extremes $P^{-3}(L_*d)$ and $P^{-4}(R_*d)$ which intersects ER_*, but $P^{-j}(\zeta)$, $j = 1, 2, 3$ do not intersect ER_* nor EL_*.

Similar results hold for an arc ζ in Γ^L with one extreme at L_*d and the other extreme point on EL_*, such that no other point in the arc is contained in EL_*

Proof. Since all proofs are similar we will only provide the proof for case 2.

Consider an arc ζ contained in $\overline{W}^s(c) \cap \Gamma^R$ with point R_*d and arc ER_* as extremes, so that no other point in the arc is contained in ER_*. By the previous proposition, pullback $P^{-1}(\zeta)$ must be a continuous arc contained in Γ^L, with extremes $P^{-1}(R_*d)$ and L_*d, which does not intersect EL_*. Pulling back this arc, we obtain a new arc $P^{-1}(P^{-1}(\zeta)) = P^{-2}(\zeta)$ in Γ^R

with extremes $P^{-2}(R_*d)$ and $P^{-1}(L_*d)$ that does not intersect ER_*; by pulling back arc $P^{-2}(\zeta)$, we obtain arc $P^{-3}(\zeta)$ in Γ^L, with ends $P^{-3}(R_*d)$ and $P^{-2}(L_*d)$. Since EL_* is a continuous arc with extremes cL_* and dL_*, and point cL_* lies between points $P^{-3}(R_*d)$ and $P^{-2}(L_*d)$, then $P^{-3}(\zeta)$ must intersect EL_*. See Figure 9. ▌

In order to describe an ejection-collision orbit which passes through a finite sequence of binary or simultaneous binary collisions, we use a sequence of symbols of the form ERLRC, that we read as a trajectory that ejects from total collision has a right–BC, a left–SBC, then another right–BC and finally goes directly to total collision.

6. MAIN RESULTS

To obtain a description of the orbits to which we associate a sequence of symbols as given in last paragraph, we define some segments contained in $\overline{W}^s(c) \cap \Gamma$, which we will call *prototype segments*.

Recall that arcs ER_* and EL_* divide half planes Γ^R and Γ^L respectively, in two regions, one being bounded, while the other is unbounded. Let us denote by Γ_1^R and Γ_1^L the bounded components of Γ^R and Γ^L determined by ER_* and EL_*, respectively; and let Γ_2^R and Γ_2^L be the unbounded components.

Definition 6. We say that a point of the form $P^{-j}(R_*d)$,$P^{-j}(L_*d)$, $P^{-j}(R_*c)$,or $P^{-j}(L_*c)$ with $j \geq 0$ is an *exterior point* if it belongs to the complement of the closure of $\Gamma_1^R \cup \Gamma_1^L$.

Let

$$J = max\{n \geq 1 \mid P^{-n}(R_*d) \in \overline{\Gamma_1^R \cup \Gamma_1^L}\}$$

and

$$K = max\{n \geq 1 \mid P^{-n}(L_*d) \in \overline{\Gamma_1^R \cup \Gamma_1^L}\}$$

Observe that $J = K$; this follows from the symmetry of the flow on the total collision manifold.

Definition 7.

1. A segment contained in $\overline{W}^s(c) \cap \Gamma^R$ having extremes on R_*d and ER_* so that no other point lies on ER_*, is said to belong to the class of *prototype–1* segments.

2. A segment contained in $\overline{W}^s(c) \cap \Gamma^R$ one of whose extremes is an exterior point and the other one lies on ER_* so that no intermediate point is contained on ER_*, is said to belong to the class of *prototype–2* segments.

3. A segment contained in $\overline{W}^s(c) \cap \Gamma^R$ is said to belong to the class of *prototype–3* segments if one of its extremes is contained in ER_* and the

other is given by $P^{-J}(R_*d)$ or $P^{-J}(L_*d)$, depending on which of them is contained in the bounded component in Γ^R determined by ER_*.

4. A segment in $\overline{W}^s(c) \cap \Gamma^L$ is called to belong to the the class of *prototype–4* segments if one of the extremes is L_*d and the other extreme lies on EL_*, so that no other point of the segment is contained on EL_*.

5. A segment contained in $\overline{W}^s(c) \cap \Gamma^L$ so that one of its extremes is an exterior point and the other extreme lies on EL_* so that no other point of the segment is contained on EL_*, is said to belong to the class of *prototype–5* segments.

6. A segment contained in $\overline{W}^s(c) \cap \Gamma^L$ is said to belong to the class of *prototype–6* segments if one of its extremes is contained in EL_* and the other one is given by $P^{-J}(R_*d)$ or $P^{-J}(L_*d)$, depending on which of them is contained in the bounded component in Γ^L determined by EL_*.

Remark 8. A segment belonging to the class of prototype-i segments will be said to belong to $Prot(i)$ and will be denoted by $Prot(i)$. Segments $Prot(2)$ and $Prot(5)$ are contained in the unbounded components, while all the others are contained in the bounded ones.

By using Proposition 3 and its Corollary 1 we obtain the existence of an infinite number of segments contained in $\overline{W}^s(c) \cap \Gamma^{R,L}$ and belonging to each one of the above defined six classes of prototype-i segments. Observe that segments belonging to the three first classes are subsets of Γ^R and those belonging to the other three classes are subsets of Γ^L. All of this reflects the geometric symmetries of the symmetric collinear four body problem and the symmetry due to the reversibility of the problem.

Now, we show some examples of segments contained in $\overline{W}^s(c)$ and belonging to each one of the classes of prototype segments.

Example 9. For examples in classes $Prot(i)$, $i = 1, 2$ we refer to Figures 6 and 12. Segment γ_1^R contained in γ^R, having one extreme at R_*d and the other extreme on ER_*, so that no other point is contained in ER_* is a segment in the class of prototype–1 segments. Segment γ_2^R contained in γ^R, with one extreme at R_*c and the other extreme on ER_* so that no other point in γ_2^R is contained in ER_* is a segment in the class of prototype–2 segments. In order to obtain an example of a prototype–3 segment consider $P^{-(J+1)}(\gamma_1^R)$; we know by Corollary 1 that this arc intersects ER_*, the example we are looking for is defined by the subsegment of $P^{-(J+1)}(\gamma_1^R)$ with one end given by $P^{-J}(R_*d)$ or $P^{-J}(L_*d)$ depending on which of these points lies on the bounded component determined by ER_* while the other end is the first intersection of $P^{-(J+1)}(\gamma_1^R)$ with ER_* and no other point in the considered segment is contained in ER_*. For a graphical representation in case $\alpha_2 < \alpha < \alpha_3$, see Figure 9, and replace segment ζ by segment γ_1^R already defined. Next, examples for $Prot(i)$,$i = 4, 5, 6$ are

TABLE 2.
Generation of prototype segments for $\boldsymbol{\alpha} \in (0, \boldsymbol{\alpha}_1) \cup (\boldsymbol{\alpha}_3, \boldsymbol{\alpha}_4)$

	generated segments					
Generator segments	*Prot(1)*	*Prot(2)*	*Prot(3)*	*Prot(4)*	*Prot(5)*	*Prot(6)*
Prot(1)	*0*	*1*	*1*	*0*	*0*	*0*
Prot(2)	*1*	*1*	*0*	*0*	*0*	*0*
Prot(3)	*0*	*0*	*0*	*1*	*1*	*0*
Prot(4)	*0*	*0*	*0*	*0*	*1*	*1*
Prot(5)	*0*	*0*	*0*	*1*	*1*	*0*
Prot(6)	*1*	*1*	*0*	*0*	*0*	*0*

defined in a symmetric way as those for $i = 1, 2, 3$. Segment γ_1^L contained in γ^L, with one extreme at L_*d and the second extreme on EL_* so that no other point in γ_1^L is contained in EL_*, is an example of a segment in the class of prototype–4 segments. Segment γ_2^L contained in γ^L with one extreme at L_*c and the other at the first intersection of γ^L with EL_*, from point L_*c, belongs to the class of prototype–5 segments. In order to obtain an example of a prototype–6 segment consider $P^{-(J+1)}(\gamma_1^L)$, we know by Corollary 5 that this arc intersects EL_*. The example we are looking for is defined by the subsegment of $P^{-(J+1)}(\gamma_1^L)$ with one end given by $P^{-J}(R_*d)$ or $P^{-J}(L_*d)$, depending on which of these points lies on the bounded component determined by EL_* while the other end is the first intersection of $P^{-(J+1)}(\gamma_1^L)$ with EL_*, and no other point in the considered segment is contained in EL_*.

THEOREM 10. *Pullbacks of segments contained in $\overline{W}^s(c) \cap \Gamma$ which belong to any of the prototype classes defined by the Poincaré Map are generated according to Tables 2 and 3 where we show how prototypes are generated when considering their inverse images, iterating P^{-1} until obtaining non empty intersection with $\overline{W}^u(d)$. Values given on the Tables depend strongly on the dynamics of the flow for different values of the parameter.*

We obtain the same Table for values of the parameter $\alpha_4 > \alpha > \alpha_3$, as the one obtained for $\alpha_1 > \alpha > 0$, but the difference lies on the fact that we need P^{-1} or P^{-4} in order to obtain non empty intersection with $\overline{W}^u(d)$, in the first case, while we need P^{-1} or P^{-2} for the second one.

TABLE 3.
Generation of prototype segments for $\boldsymbol{\alpha} \in (\boldsymbol{\alpha}_2, \boldsymbol{\alpha}_3)$

	Generated segments					
Generator segments	*Prot(1)*	*Prot(2)*	*Prot(3)*	*Prot(4)*	*Prot(5)*	*Prot(6)*
Prot(1)	*0*	*0*	*0*	*0*	*1*	*1*
Prot(2)	*1*	*1*	*0*	*0*	*0*	*0*
Prot(3)	*0*	*0*	*0*	*0*	*1*	*1*
Prot(4)	*0*	*1*	*1*	*0*	*0*	*0*
Prot(5)	*0*	*0*	*0*	*1*	*1*	*0*
Prot(6)	*1*	*1*	*0*	*0*	*0*	*0*

Observe that a prototype–i segment generates two segments, belonging to different prototype classes. In the table, we associate 1 or 0 to the row $Prot(i)$, in the column $Prot(k)$, meaning that it generates or not a segment in the class $Prot(k)$.

Proof. We will prove only some cases, since the other ones can be proved in a similar way.

1. Case $\alpha_2 < \alpha < \alpha_3$: Let $Prot(1)$ be an arc belonging to the class of prototype–1 segments, contained in $\Gamma^R \cap \overline{W}^s(c)$ with one extreme at $R_* d$ and the other on ER_* so that no other point is contained in ER_*. Observe that $P^{-j}(Prot(1)), j = 1, 2$ do not intersect $ER_* \cup EL_*$, but $P^{-3}(Prot(1))$ does intersect EL_* and by Proposition 4, is an arc with extremes at $P^{-2}(L_* d)$ and $P^{-3}(R_* d)$. As a consequence, $P^{-3}(Prot(1))$ intersects EL_* in one point and therefore generates one prototype–5 segment and a prototype–6 segment.

2. The argument we give for prototype–2 is valid for every mass parameter. If we consider a $Prot(2)$, which is an arc in $\Gamma^R \cap \overline{W}^s(c)$ with one extreme at an exterior point, say A and the other extreme on ER_* so that no other point is contained in ER_*, by Proposition 4, $P^{-1}(Prot(2))$ is an arc in Γ^R joining $P^{-1}(A)$ and $R_* d$, so it must intersect arc ER_*. So we have generated a prototype–2 segment and a prototype–1 segment, since the intersection $P^{-1}(Prot(2)) \cap ER_*$ is assumed to contain only one point.

3. Case $\alpha_2 < \alpha < \alpha_3$: Let $Prot(3)$ be a prototype–3 segment which joins $P^{-2}(R_* d)$ and a point in ER_*, so that no other point of the segment is contained in ER_*. According to Proposition 4, $P^{-1}(Prot(3))$ is an arc

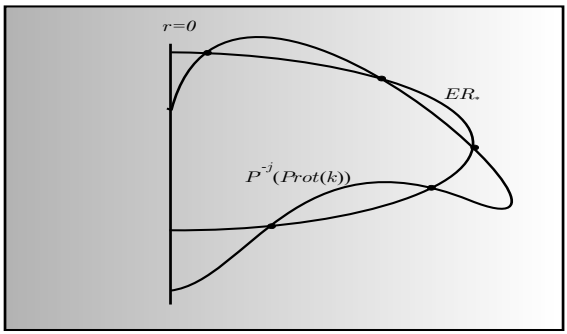

FIG. 10. Points having the same sequence of BC.

joining $P^{-1}(P^{-2}(R_*d)) = P^{-3}(R_*d)$, that is an exterior point lying in Γ^L, and L_*d. So, $P^{-1}(Prot(3))$ must intersect EL_* in one point, generating in this way one prototype–5 segment and one prototype–4 segment.

∎

We must observe that while for any value of the parameter, segments in classes 2, 3, 5 and 6 only need one application of P^{-1} to obtain a non empty intersection with ER_* or EL_*, the number of applications of P^{-1} needed for segments in classes 1 and 4 to intersect ER_* or EL_* depend on the values of the parameter. If $\alpha_1 < \alpha < \alpha_2$ then prototype–1,4 segments need two applications of P^{-1}. If $\alpha_2 < \alpha < \alpha_3$ then prototype–1,4 segments need three applications of P^{-1} and in the case $\alpha_3 < \alpha$, prototype–1,4 segments need four applications of P^{-1}.

It may happen that the cardinality of the number of points in the intersection $P^{-j}(Prot(k)) \cap ER_*$ or $P^{-j}(Prot(k)) \cap EL_*$ is bigger than one. In this case, orbits corresponding to each one of these points have associated the same sequence of symbols R and L between ejection and total collision. Assuming that m points are contained in the intersection, we obtain $m-1$ different segments in $P^{-j}(Prot(k))$ whose extremes lie in ER_* or EL_*; and the pullback of each of these segments transforms them in loops with extremes on R_*d or L_*d, and the pullbacks of these loops do not generate new intersections with ER_* neither with EL_*. That is why we can assume, without loss of generality that pullbacks of $P^{-j}(Prot(k))$ only intersect ER_* or EL_* in one point, since no new sequence of symbols is obtained. See Figure 10.

DEFINITION 11. A point $p \in \overline{W}^s(c) \cap \overline{W}^u(d) \cap \Gamma$ is said to be a *first ejection-collision point* if the orbit through this point comes directly from total collision without experiencing a binary or a simultaneous binary col-

lision in between. In the same way, a point $p \in \overline{W}^s(c) \cap \overline{W}^u(d) \cap \Gamma$ is called a *last ejection-collision point* if the orbit through this point goes directly to total collision without experiencing a binary or a simultaneous binary collision in between.

Next, we show how to use Tables 2 and 3 given in Theorem 10 to generate a family of ejection–collision orbits that have a finite sequence of binary or simultaneous binary collisions. In order to do this, we begin by analyzing the pullbacks of prototype segments contained in γ^R and γ^L. We describe now families of ejection-collision orbits that show distinct dynamics.

The following result shows the existence of a family of ejection–collision orbits having n–binary collisions or n–simultaneous binary collisions for $n \geq 1$. It is clear that they are different from the homothetic orbit, which is free from collisions.

PROPOSITION 12. *For any value of the parameter α, for each $n \geq 1$, there exist a type ER^nC orbit, and a type EL^nC orbit.*

Proof. We will prove the existence of the family of orbits having related sequences given by ER^nC, since the existence of the other family is proved in a symmetric way.

We know that points contained in $\gamma^R \cap \sigma^R$ are first and last ejection–collision points, so their orbits have associated sequences of the form ERC. When considering subsegment γ_2^R of γ^R, its pullback $P^{-1}(\gamma_2^R)$ intersects ER_*, and generates two segments, one of prototype–1, and one of prototype–2; through the point of intersection of $P^{-1}(\gamma_2^R)$ with ER_* (remember we are assuming there is only one intersection point) passes an orbit with associated sequence $ERRC$. According to Theorem 10, the new prototype–2 segment, under P^{-1} intersects ER_* and generates another prototype–1 segment and a prototype–2 segment, and to the common point of these two resulting segments corresponds an orbit with a sequence of the form $ERRRC$. Continuing this process of iterating all prototype–2 segments obtained at each step, it is possible to construct the desired family of orbits. ∎

PROPOSITION 13. *For $0 < \alpha < \alpha_1$, there are ejection-collision orbits which perform a sequence of n ($n \geq 1$) binary and/or simultaneous binary collisions.*

Proof. As we know, arcs γ^R and σ^R in Γ^R, contained in $\overline{W}^s(c)$ and $\overline{W}^u(d)$, respectively, intersect, generating two segments, one prototype–1 segment and one prototype–2 segment: γ_1^R and γ_2^R, which are subsegments of γ^R and their common point, which is unique by assumption, is a first and last ejection-collision point. By Theorem 10, by iterating these two prototype segments under P^{-1}, we obtain according to Table 2, four prototype segments : say, one $Prot(2)$ and one $Prot(3)$ for γ_1^R and, one $Prot(1)$ and

$Prot(2)$ for γ_2^R and two first and last ejection-collision points, given by the common point of each one of the pairs of the given prototype segments, as two ejection-collision orbits having three and two binary and simultaneous binary collisions, respectively. This way, we can continue this process of iteration of P^{-1} for each one of the obtained four prototype segments. This is possible due to Theorem 10. Each of the four segments need to be iterated, under P^{-1}, once or twice in order to obtain a non empty intersection with ER_* or EL_*.

So, we can assume that we have an orbit with associated sequence given by $EQ_1Q_2 \dots Q_nC$, where $Q_i \in \{R, L\}$; moreover, the last symbol Q_n before total collision was obtained through two prototype segments, say $Prot(k)$ and $Prot(j)$. Iterating one of these two prototype segments we can obtain a new trajectory having one or two last new symbols Q_{n+1}, or $Q_{n+1}Q_{n+2}$. This depends on whether we require one or two iterations under P^{-1} of the given prototype segments, in order to obtain a non empty intersection with ER_* or EL_*. Then we have obtained an orbit with associated sequence of symbols given by

$$EQ_1Q_2 \dots Q_nQ_{n+1}C \quad \text{or} \quad EQ_1Q_2 \dots Q_nQ_{n+1}Q_{n+2}C.$$

∎

COROLLARY 14. *For $0 < \alpha < \alpha_1$, there are ejection-collision orbits of the type $ERLRC$. By symmetry, orbits of the type are $ELRLC$ are obtained .*

Proof. Consider the segment γ_1^R contained in γ^R. By Theorem 10, its pullback $P^{-1}(\gamma_1^R)$, does not intersect ER_* nor EL_*, but $P^{-2}(\gamma_1^R)$ does intersect ER_*, obtaining a prototype–2 and a prototype–3 segment, and the common point is a first ejection-collision point. Iterating this point under P, we have that the first iteration is a point in Γ^L and the second one is a point in Γ^R, which is a last ejection-collision point. So, to these three points corresponds an orbit with associated sequence given by $ERLRC$. ∎

COROLLARY 15. *The following statements hold.*

1.For $\alpha_2 < \alpha < \alpha_3$, there are ejection-collision trajectories with $ELR\,LRC$ as associated sequence, and by symmetry, trajectories with sequences $ERLRLC$ are obtained.

2.For $\alpha_3 < \alpha$, there are ejection-collision trajectories with associated sequences $ERLRLRC$, and by symmetry, trajectories with sequences $ELRL\,RLC$ are obtained.

Proof.

1. Consider segment γ_1^R; contained in γ^R, according to Table 2, the pullbacks $P^{-1}(\gamma_1^R)$, and $P^{-2}(\gamma_1^R)$ do not intersect neither ER_* nor EL_*, but $P^{-3}(\gamma_1^R)$ does intersect EL_*, obtaining a prototype–5 and a prototype–6 segment and a first ejection–collision point p. Iterating this first ejection–collision point under P we obtain that its first iteration give us a point in Γ^R; the second iteration of the point lies in Γ^L and the third iteration gives us a last ejection–collision point contained in Γ^R. So, we can associate a sequence of the form $ELRLRC$ to point p. The existence of the other orbit with associated sequence $ERLRLC$ is obtained by symmetry.

2. The proof of this part is completely similar to the above one.

∎

In order to end this section, we give an interpretation to sequences of symbols of the form $EQ_1Q_2 \dots Q_j \dots Q_mC$, with $Q_j \in \{R, L\}$, which are associated to ejection-collision trajectories having a finite set of binary or simultaneous binary collision in terms of the original coordinates x, y for the symmetric collinear four body problem.

Recall that binary and simultaneous binary collisions correspond to $x = 0, y \neq 0$ and $y = \sqrt{\alpha}x \neq 0$, respectively. Under the McGehee transformation these singularities correspond to values of θ given by $\theta = \pi/2$ and $\theta = \theta_\alpha$, respectively. So, when in McGehee coordinates $\theta = \pi/2$, we have a binary collision of the inner pair of the collinear configuration, while having $\theta = \theta_\alpha$ means that we have a simultaneous binary collision. Observe that we did not consider the case $x = y = 0$, because in this case total collision occurs.

Taking into account this information, and the fact that to symbol L corresponds a point in Γ^L, then an orbit where a symbol $Q_j = L$ appears in its associated sequence $EQ_1Q_2 \dots Q_j \dots Q_mC$, performs a simultaneous binary collision when crossing Γ^L. In the case symbol $Q_j = R$ appears in the sequence, then a binary collision of the inner pair occurs at the time the orbit crosses Γ^R.

In this way, sequences ER^nC and EL^nC obtained in Proposition 12 for any value of α, are associated to ejection-collision orbits that either have a sequence of n simultaneous binary collisions or a sequence of n binary collisions of the inner pair, respectively. A similar interpretation of the sequences $ERLRC$ and $ELRLC$ obtained in Corollary 14, can be given, as we see in Figure 11.

Next, we give a description of orbits, not necessarily ejection-collision orbits which pass through a sequence of binary or simultaneous binary collisions. In order to do this, we shall study iterations, under the inverse P^{-1} of the Poincaré Map of regions, instead of segments, as done in [3] and [1]. The regions are contained in $\Gamma = \Gamma^R \cup \Gamma^L$, which has been our convenient

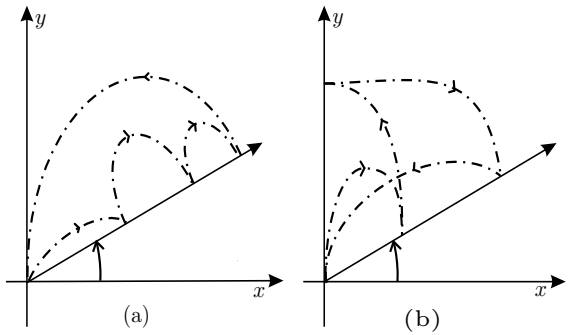

FIG. 11. Ejection-collision orbits : (a) EL^3C y (b) $ELRLC$.

Poincaré section. The Poincaré map will give us global information about possible sequences of binary or simultaneous binary collisions an orbit can have.

We will define a finite set of regions $R_i, i = 1, \ldots, 2N$ ($N = 4$ for $0 < \alpha < \alpha_1$, $N = 5$ for $\alpha_2 < \alpha < \alpha_3$ and $N = 6$ for $\alpha_3 < \alpha < \alpha_4$) ; all of them, but two, are contained in $\overline{\Gamma_1^R \cup \Gamma_1^L}$. The remaining two regions will be the unbounded regions $\Gamma_2^R$and Γ_2^L.

Define N first regions R_i, $i = 1, \ldots, N$ in Γ^R. The other N regions R_i, $i = N+1, \ldots, 2N$ in Γ^L will be defined by symmetry. The first $N-1$ regions in Γ^R are contained in $\overline{\Gamma_1^R}$, while last region R_N in Γ^R is just Γ_2^R, the unbounded part of Γ^R determined by ER_*, and R_{2N} is the unbounded region Γ_2^L.

Region R_1 is the region in Γ_1^R, bounded by ER_*, line segment in $r = 0$ between points dR_* and R_*d, and the segment γ_1^R; region R_{N+1} is the region in Γ_1^L, bounded by EL_*, the line segment in $\{r = 0\}$, between points dL_* and L_*d and the segment γ_1^L. To define regions $R_i, i = 2 \ldots N-2$, we shall consider a finite set of pullbacks of segments $\gamma_1^R \subset \gamma^R$ and $\gamma_1^L \subset \gamma^L$. We define regions R_2 to R_{N-2} and R_{N+2} to R_{2N-2} for each one of the intervals where parameter α is contained. We make use of Corollary 5 and the symmetry of the flow in the considered cases for the values of the parameter.

1. For $0 < \alpha < \alpha_1$(i.e $N = 4$). Observe $P^{-1}(\gamma_1^L) \subset \Gamma_1^R$ does not intersect ER_*, but $P^{-2}(\gamma_1^L)$ does intersect ER_*. So, we define region R_2 as the region in Γ_1^R bounded by $P^{-1}(\gamma_1^L)$ and the segment in $\{r = 0\}$ between points R_*d and $P^{-1}(L_*d)$; region $R_{N+2} = R_6$ is the region symmetric to R_2, contained in Γ_1^R; that is, the region bounded by $P^{-1}(\gamma_1^R)$ and the segment in $r = 0$ between points L_*d and $P^{-1}(R_*d)$.

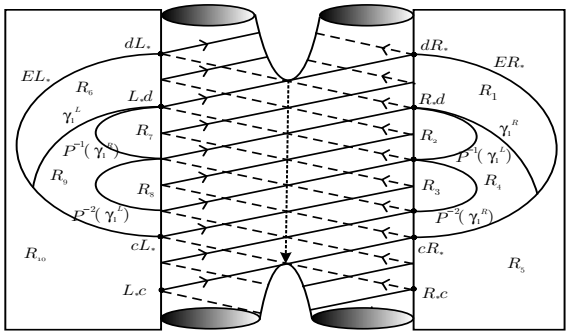

FIG. 12. Basic regions $R_i, i = 1 \dots 10$, in Γ^R for $\alpha_2 < \alpha < \alpha_3$.

2. For $\alpha_2 < \alpha < \alpha_3$, (i.e. $N = 5$). Define regions R_2, R_{N+2} in the same way as we did in last case. Observe that $P^{-2}(\gamma_1^R) \subset \Gamma_1^R$ and $P^{-2}(\gamma_1^R)$ does not intersect ER_*; in the same way, $P^{-2}(\gamma_1^L) \subset \Gamma_1^L$ and $P^{-2}(\gamma_1^L)$ does not intersect EL_*. But $P^{-3}(\gamma_1^R)$ intersects EL_* and $P^{-3}(\gamma_1^L)$ intersects ER_*. So, we define region R_3 as the region bounded by $P^{-2}(\gamma_1^R)$ and $\{r = 0\}$ and region $R_{N+3} = R_8$ as the region bounded by $P^{-2}(\gamma_1^L)$ and $\{r = 0\}$. See Figure 12.

3. For $\alpha_3 < \alpha < \alpha_4$ (i.e. $N = 6$), Define R_2, R_3 and R_{N+2}, R_{N+3} as we did in the previous case. Observe that $P^{-3}(\gamma_1^R)$ does not intersect EL_* nor $P^{-3}(\gamma_1^L)$ intersects ER_*; but $P^{-4}(\gamma_1^R)$ intersects ER_* and $P^{-4}(\gamma_1^L)$ intersects EL_*. So we define region R_4 in Γ_1^R as the region bounded by $P^{-3}(\gamma_1^L)$ and the line $\{r = 0\}$ and region $R_{N+4} = R_{10}$ is defined as the region in Γ_1^L bounded by $P^{-3}(\gamma_1^R)$ and the line $\{r = 0\}$.

Region R_{N-1} is given by the complement of $\bigcup_{j=1,\dots,N-2} R_j$ in Γ_1^R and region R_{2N-1} is the complement of $\bigcup_{j=N+1,\dots,2N-2} R_j$ in Γ_1^L . See Figure 12 for case $N = 5$. As it was established, those N regions in Γ^L are defined in a symmetric way as regions in Γ^R were defined.

We study how these regions are mapped one to another under P^{-1}. To do this consider an alphabet $\mathcal{A} = \{R_i\}_{i=1,\dots,2N}$ of $2N$ symbols, to each one of them corresponds one of the $2N$ regions $R_i, i = 1, \dots, 2N$, already defined. We shall study how the dynamics among these regions under P^{-1} works.

DEFINITION 16. A *transition matrix* is a matrix $A = (a_{ij}) \in M_{2N\times 2N}$, so that $a_{ij} = 1$ if region R_i is mapped to region R_j under P^{-1}, and $a_{ij} = 0$, otherwise.

Transition matrices determine all admissible transitions between symbols R_i.

DEFINITION 17. The *transition graph* G_A, associated to a transition matrix A is the directed graph with $2N$ different vertices, which by simplicity are denoted by i, $i = 1, \ldots, 2N$ and some directed arrows. We have a directed arrow from vertex i to vertex j if $a_{ij} = 1$; in case $a_{ij} = 0$, there is no connection from vertex i to vertex j.

Our objective is to determine a transition matrix A, which describes the dynamics of the regions R_i, for a given range of values of the parameter and its associated transition graph. This permits to know the dynamics of the orbit beginning in a given region in terms of its sequence of binary and simultaneous binary collisions. We will use all of the previously obtained information

THEOREM 18. *Transition matrices for the symmetric collinear four body problem are given by matrices of the form*

$$A = \begin{pmatrix} C & D \\ D & C \end{pmatrix} \in M_{2N\times 2N},$$

where

$$C = \begin{pmatrix} 0 & \ldots & 0 & 0 & 0 \\ \vdots & \ddots & 0 & 0 & 0 \\ 0 & 0 & 0 & 0 & 0 \\ 0 & 0 & 0 & 0 & 0 \\ 1 & 0 & \ldots & 0 & 1 \end{pmatrix}, \; D = \begin{pmatrix} 0 & 1 & 0 & \ldots & 0 \\ \vdots & 0 & \ddots & 0 & 0 \\ \vdots & 0 & 0 & 1 & 1 \\ 0 & 0 & 0 & 1 & 1 \\ 0 & \ldots & \ldots & 0 & 0 \end{pmatrix} \in M_{N\times N}$$

and $N = 4$ *corresponds to* $0 < \alpha < \alpha_1$, $N = 5$ *corresponds to* $\alpha_2 < \alpha < \alpha_3$ *and* $N = 6$ *corresponds to* $\alpha_3 < \alpha < \alpha_4$.

Proof. The pullback of region R_N is obtained as follows. The argument for any of the three cases is the same. So we consider any of $N = 4, 5$, or 6. All considered points lie in R_N. The pullback of a point in R_N near cR_* pass near R_*c and the pullback of a point in the region, close to ER_*, must be close to R_*d. Analogously, points close to dR_*, under P^{-1}, go to points near R_*d. So, $P^{-1}(R_N)$ intersects R_1 and R_N. Pullbacks for the others regions are determined in a similar way. ∎

COROLLARY 19. *Transition graphs between regions are given in Figure 13.*

The proof follows from Theorem 18 and is omitted.

Observe that symmetries appearing in all transition matrices and their associated transition graphs reflect the geometric symmetries of the collinear configuration.

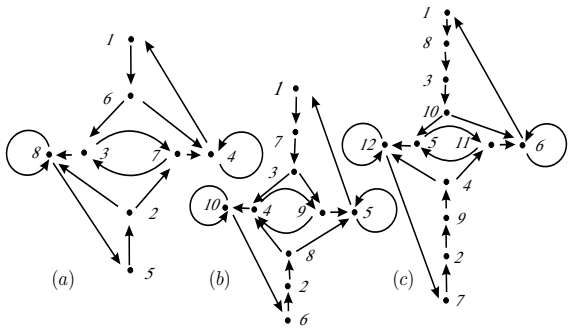

FIG. 13. Transition graph G_A between regions for (a) $0 < \alpha < \alpha_1$,, (b) $\alpha_2 < \alpha < \alpha_3$, and (c) $\alpha_3 < \alpha < \alpha_4$.

7. ACKNOWLEDGMENTS

M. Medina would like to acknowledge to J. Delgado and S. Kaplan for their encouragements and so many discussions which turned out to be very useful to clarify many ideas. This work was partially supported by CONACYT grant 32167-E.

REFERENCES

1. S. Chesley and K. Zare, *Order and chaos in the planar isosceles three body problem* , In Chaos and irreversibility (Budapest, 1997). Chaos **8** (1998), Number 2, 475–494.

2. J. Delgado and M. Álvarez-Ramírez, *Blow-up of the planar 4-body problem with an infinitesimal map*, Discrete and Continuous Dynamical Systems **9**, Number 5, (2003), 1149–1173.

3. Sam Kaplan, *Symbolic dynamics of the collinear three body problem*, in Geometry and Topology in Dynamics (Winston-Salem, NC,1998/San Antonio TX), Contemp. Math. **246**, 143–162.

4. R. McGehee, *Triple collision in the collinear three body problem*, Invent. Math. **27**, (1974), 191–227.

5. C. Simó and E.A. Lacomba, *Analysis of some degenerate quadruple collisions*, Celestial mechanics **28**, (1982), 49-62.